Direct determination of atomic positions on the Cu(110)-(1×2)-H surface

A. V. Mijiritskii,* U. Wahl,† M. H. Langelaar, and D. O. Boerma
Nuclear Solid State Physics, Materials Science Centre, University of Groningen, Nijenborgh 4, 9747 AG Groningen, The Netherlands
(Received 17 September 1997)

Results of a low-energy ion scattering study of the H-induced 1×2 reconstruction of the Cu(110) surface are presented. The surface was bombarded with 6-keV Ar^+ ions under a grazing angle of 5°, 6°, or 8°; azimuthal scans of the yields of the scattered Ar and recoiled Cu and H atoms emitted at a scattering angle of 45° were measured. The scans were compared with the results of computer simulations. We confirm that the surface is of the 1×2 ''missing-row'' type. Nine possible positions of H atoms at the Cu(110)-(1×2) surface for different coverages were analyzed. The H atoms were found to be situated in one of the two possible trigonal hollow sites on the missing-row reconstructed surface. To obtain good fits to the experimental data, large thermal vibration amplitudes of the H atoms had to be assumed. These large amplitudes can be due to a nonharmonic potential. [S0163-1829(98)05315-6]

I. INTRODUCTION

The interaction of hydrogen with transition-metal surfaces is of great interest due to a variety of applications such as catalysis,[1] hydrogen storage,[2] enhanced Cu reflow in microelectronics,[3] and nuclear fusion technology.[4] From a more fundamental point of view, because of its simplicity, hydrogen on a metal surface is a good model system to study electron and phonon interactions and to observe quantum effects.[5–9] Determination of the geometry of the adsorbed layer in a given chemisorption system provides important information for understanding the nature of H-substrate bonds. The H-covered Cu(110) surface is one of these systems. In contrast to other fcc metal (110) surfaces such as Ni(110) or Pt(110), H adsorption on Cu(110) is an activated process, i.e., the sticking coefficient for molecular hydrogen H_2 is negligible compared to the one for atomic hydrogen H.[10] Experimental studies of H-covered Cu(110) therefore require one to expose the surface to atomic H, which is usually produced by means of hot W filaments or tubes. During the past 15 years a number of studies on the hydrogen-induced reconstruction of the Cu(110) surface has been reported.[7,11–18,20] Most of them agreed on the fact that at deposition temperatures below about 100 K and H exposures in the approximate range 2–8 L (1 L=1×10^{-6} Torr s) the Cu(110) surface undergoes a $(1\times3)_H$ reconstruction. Higher exposures lead to a transition from the $(1\times3)_H$ to the $(1\times2)_H$ reconstruction. The $(1\times2)_H$ reconstruction can also be produced either by H deposition at higher temperatures or by heating a $(1\times3)_H$ sample to above about 150 K.[11] On annealing to temperatures above 300 K, de-reconstruction $(1\times2)_H\rightarrow1\times1$ with the simultaneous desorption of H_2 takes place. Note that, with the exception of Ref. 10, most experimentalists could not measure the exact exposure to atomic H and have only given values for the exposure to the mixture H + H_2 of atomic and molecular hydrogen. Since this mixture varies according to specific experimental conditions, quoted expositions are only rough indications. The same holds for the temperatures given above, which can vary somewhat due to different heating rates.

Earlier experimental studies using photoemission spectroscopy[13–16] or He and Ne diffraction[12] and also older theoretical works[17,18] indicated that subsurface reconstructions of Cu (Ref. 12) and also subsurface sites of H (Refs. 13–16) might be involved in Cu(110)-(1×2)-H. From 1.5-keV He ion scattering spectroscopy, however, it could be proven, that the Cu(110)-(1×2)-H reconstruction is of the missing-row type,[19] which was also confirmed by more recent theoretical considerations.[21,20] Concerning the adsorption sites of H, studies combining low-energy electron diffraction (LEED) with electron-energy-loss spectroscopy[7,11] (EELS) were in accordance with H in trigonal hollow surface sites. Theoretical calculations using the effective-medium theory also suggest this site to be the most stable site of **H** on Cu(110).[20] A direct determination of the H adsorption site has been lacking so far.

Low-energy ion scattering measurements are especially suited to give direct information on the position of light adsorbate atoms on surfaces.[5,22,23] In the following we present an analysis of eight possible surface sites[22] and a subsurface site[20] for H atoms on a 1×2 missing-row surface.

II. EXPERIMENTAL METHODS

A. Experimental setup and sample preparation

The measurements were carried out in a low-energy ion scattering (LEIS) time-of-flight (TOF) system described earlier.[24] The ultrahigh vacuum part consists of a main chamber and a preparation chamber, both with a base pressure of 2×10^{-10} mbar. In the present work, we used a pulsed beam of 6-keV Ar^+ ions and TOF spectra of scattered and recoiled particles were measured. The combined yield of both neutral atoms and ions was detected. In this way, the angular scans are not influenced by charge-exchange effects. At the same time, this makes the measurements sensitive not only to the outer surface layer, but to the first few layers as well. The sample to be investigated was fixed onto a goniometer allowing rotation around three perpendicular axes. The orientation of the sample was driven by computer-controlled stepping motors.

The atomic hydrogen source[25] consists of a thin tungsten tube with an inner diameter of 0.5 mm connected to a bellows system, so that it can be positioned near the sample surface. The tube was heated by means of electron bombardment to approximately 1800 K and its temperature was measured by means of a pyrometer. A beam of atomic H was produced by leading H_2 gas through this tube.

A Cu single crystal was cut along a (110) plane with an acid saw. Then it was mounted on the goniometer of a polishing machine and oriented using x-ray diffraction. In this way a (110) face could be polished with a misorientation of less than 0.1°. The sample was transferred into the preparation chamber and subjected to baking at about 500 °C for several hours to remove impurities. Subsequently, it was subjected to sputtering (2-keV Ar^+, 150 °C for 20 min) and annealing (250 °C for 20 min) cycles in order to obtain a clean well-ordered (110) surface. Each preparation step was followed by LEED and LEIS analysis of the sample surface performed in the main chamber. In all cases LEED showed sharp 1×1 patterns with a low background at the final stage, and no contamination could be observed with LEIS.

The hydrogen deposition was carried out in the main chamber. During the deposition, the $H+H_2$ pressure was kept at about 2×10^{-8} mbar (uncorrected pressure reading from the ionization gauge) and the sample temperature at approximately 240–250 K. Under these conditions exposition to $(2-3)\times10^{-6}$ mbar s=1.5–2.3 L was found to result in both a saturation of hydrogen coverage visible with LEIS (Ref. 26) and a sharp LEED pattern. After deposition the sample temperature was lowered to 130–150 K and LEIS scans were measured. Following a complete azimuthal LEIS scan, LEED was showing only slightly weaker 1×2 spots. This was in accordance with the H recoil yield from LEIS itself, which, for a fixed azimuthal and polar incidence angle, indicated only H losses around 5–6 % due to sputtering and desorption during the scan.

B. Measurements and computer simulations

A scheme of the geometry during the experiments is given in Fig. 1 (top). To probe the surface structure, a grazing incident beam direction was chosen with an incoming (polar) angle $\alpha=5°$, 6°, or 8° with respect to the sample surface. The scattering angle was $\theta=45°$. The azimuthal scans were taken by measuring the TOF spectra every 2° with the same amount of beam charge. In this geometry, the TOF peaks of recoiled H and Ar scattered from Cu were well separated, while the peak of recoiled Cu was interfering with the low-energy tail of the Ar peak (see Fig. 1, bottom). To extract the Cu azimuthal scans, the Ar low-energy tail was fitted with an exponential function and subtracted from the Cu signal. Doing azimuthal LEIS scans it is very important to exactly keep the polar orientation of the sample with respect to the incoming ion beam and the detector. In that respect even offsets smaller than 1° between the rotation axis of the goniometer and the sample normal, which can hardly be avoided, present severe problems if not corrected for. A procedure how to precisely determine such offsets and to obtain exact crystal orientations with a three-axis goniometer has been described by Dygo *et al.*[27] Recording the backscattering signal from a 15-keV H^+ beam, we used their recipe in order to obtain the precise orientation of the Cu crystal when mounted in the goniometer of the LEIS chamber. Note that this procedure had to be carried out only once since the sample can be transferred between the preparation chamber and goniometer in a reproducible way.

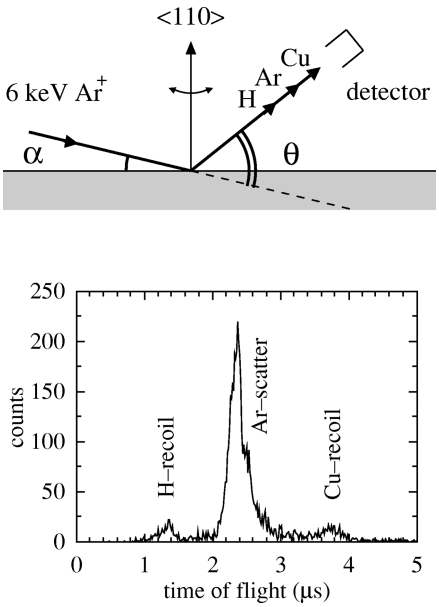

FIG. 1. Geometry of the experiments (top). Typical TOF spectrum: 6-keV Ar^+ beam, incoming (polar) angle $\alpha=8°$, scattering angle $\theta=45°$, and azimuthal angle $\phi=81°$ (bottom).

The azimuthal scans for recoiled H and Cu and for scattered Ar were simulated using the recently developed computer program MATCH. A detailed description of the program is given elsewhere.[28] In the simulations a slab was defined, with an area equal to a surface spanned by thirty-two 1×2 or eight 2×4 unit cells of the reconstructed Cu(110) surface and a thickness of three layers. The interactions of both beam and recoiled particles with the surface slab including the H atoms were taken into account. The simulation consisted of three separate stages: (i) calculation of incoming trajectories of the projectiles and created recoiled particles, in which the projectile or recoil coordinates and velocities are stored in case an atom is encountered at short distance; (ii) calculation of outgoing trajectories of H, Cu, and Ar in time-reversed mode; in which a large energy range is divided into discrete energy intervals and the medium energy of an interval is then chosen as the initial energy of the particle (all the energy losses are calculated after each collision and added to the energy of the particle); and (iii) matching of incoming and outgoing trajectories at the positions of hard collisions with a tolerance in energy corresponding to the chosen energy interval and a small tolerance in the distance of the in- and out-going trajectories. The matches are weighted proportionally to (a) the probability for an atom to be at the proper position to cause the scattering or recoiling event and (b) the differential scattering or recoiling cross section of the collision.

All trajectories were calculated in three-dimensional space. The thermal vibrations were included by performing the calculations for many (>500) ''frozen lattices'' and adding the results. A frozen lattice was obtained by displacing the atoms from their equilibrium positions over a distance chosen from a Gaussian thermal displacement distribution. All calculations were carried out in the quasibinary collision

TABLE I. Values for the parameters found in this work.

screening length reduction factor	Ar-Cu, 0.92 ± 0.03; Cu-Cu, 0.90;[a]
of the universal potential	Ar-H, 0.85 ± 0.03; Cu-H, 0.85[a]
buckling of the topmost copper layer (Å)	
along the y axis	<0.1
along the z axis	<0.1
atomic position of the H atom with respect	$x=1.28\pm0.04$
to the Cu(0;0;0) atom[b] (Å)	$y=1.09\pm0.07$
	$z=0.08\pm0.09$[c]
thermal vibration amplitudes of Cu atoms[d] (Å)	
first-layer atoms	$a_{x1}^{Cu}=0.09\pm0.02$
	$a_{y1}^{Cu}=0.09\pm0.02$
	$a_{z1}^{Cu}=0.11\pm0.02$
second- and third-layer atoms	$a_{x,y,z}^{Cu}=0.07\pm0.02$
thermal vibration amplitudes of H atoms[d] (Å)	$a_{x}^{H}=0.34\pm0.05$
	$a_{y}^{H}=0.37\pm0.05$
	$a_{z}^{H}=0.43\pm0.06$

[a]These adopted values resulted in good fits.
[b]The Cu(0,0,0) designates an atom in the topmost missing-row layer.
[c]The z axis is directed out of the sample.
[d]At $T=140$ K.

approximation using the Ziegler-Biersack-Littmark[29] screened universal potential. The (impact-parameter-dependent) electron stopping was included by applying the Oen-Robinson model.[30] The screening lengths of the universal potential for Ar-Cu and Cu-Cu collisions were determined by performing computer simulations for the known structure of the clean Cu(110) surface. The widths of atomic Cu position distributions due to thermal vibrations reported by Dürr *et al.*[31] and Copel *et al.*[32] were used as a starting point. These values were adjusted to give better fits. The amplitudes found are presented in Table I. The values given by Dürr *et al.*[31] and Copel *et al.*[32] are equal within the error bar to our values. The interplanar distances as determined by Copel *et al.*[32] for the clean surface and by Baddorf *et al.*[33] for the H-covered surface were adopted. The resulting lengths for the Ar-H and Cu-H interactions were determined by fitting the H-recoil scans. The obtained data are listed in Table I. From the simulations we found that at small incident angles a projectile often undergoes more than 30 ''soft'' collisions with sample atoms before it is scattered in a ''hard'' collision under a relatively large angle. It seems that an incoming projectile ''hovers'' over the sample surface for a long time and its trajectory is slightly bent after each soft impact. The influence of H atoms on the Cu-recoil and Ar-scatter azimuthal scans was found to be negligible, implying that the observed surface channeling at small incident angles can be considered to be only due to Ar-Cu interactions.

III. EXPERIMENTAL RESULTS AND DISCUSSION

A. 1×2 reconstruction

The azimuthal scans of recoiled Cu and scattered Ar atoms measured for 8° for the clean and 1×2 reconstructed Cu(110) surface are presented in Fig. 2. A clear difference in the scans for the unreconstructed and reconstructed surfaces is observed, especially in the Cu-recoil scans. The spectra can be easily understood in terms of shadowing cones as explained in Fig. 3. For small incoming angles and certain azimuthal directions, Cu atoms are shadowed from the ions by neighboring atoms, resulting in a low detected yield. In between these minima, focusing effects influence the height of the maxima in the yield. The measured (solid line) and fitted (dashed line) azimuthal scans of Cu atoms recoiled from the reconstructed surface for 6° and 8° incoming angles are shown in Fig. 3. For a fixed polar angle of the detector, a number of shadowing dips can be distinguished. The azimuthal positions of these dips correspond exactly to the real-space surface string directions. An Ar-scatter azimuthal scan calculated and fitted to the experimental data for 5° incoming

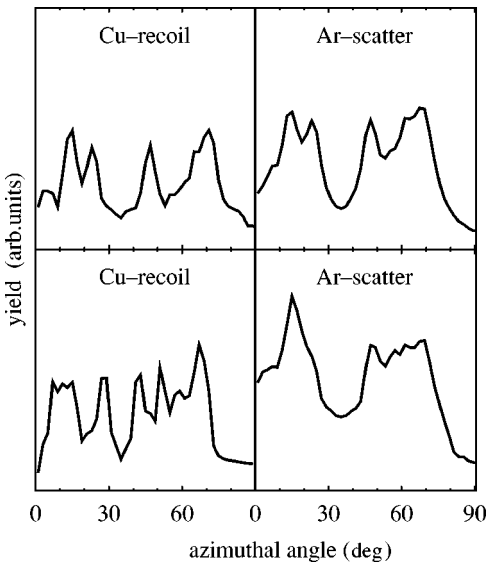

FIG. 2. Cu-recoil and Ar-scatter azimuthal scans corresponding to the 1×1 unreconstructed (top frames) and 1×2 reconstructed (bottom frames) Cu(110) surface for $\alpha=8°$. Azimuthal angles of 0° and 90° correspond to the [100] and [011] crystallographic directions, respectively.

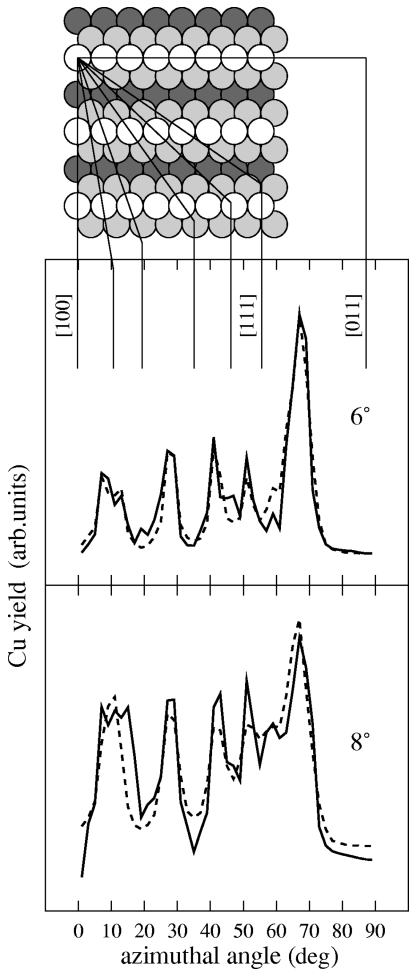

FIG. 3. Interpretation of LEIS-TOF azimuthal scans for the 1×2 missing-row reconstructed surface in terms of shadowing effects. The fits of the simulated (dashed line) Cu-recoil azimuthal scans to the experimental data (solid line) for $\alpha=6°$ and 8° are shown. Azimuthal angles of 0° and 90° correspond to the [100] and [011] crystallographic directions, respectively.

angle is shown in Fig. 4. Good agreement between experimental and calculated data was found. The simulated scans plus a small constant background were fitted to the experimental data. The remaining small differences in measured

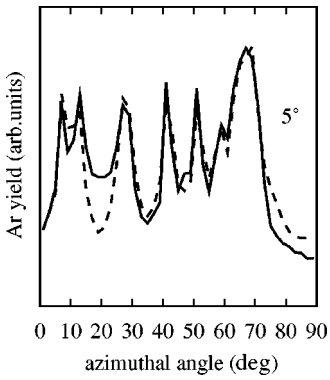

FIG. 4. Simulated Ar-scatter azimuthal scan fitted (dashed line) to the experimental data (solid line) for $\alpha=5°$. Azimuthal angles of 0° and 90° correspond to the [100] and [011] crystallographic directions, respectively.

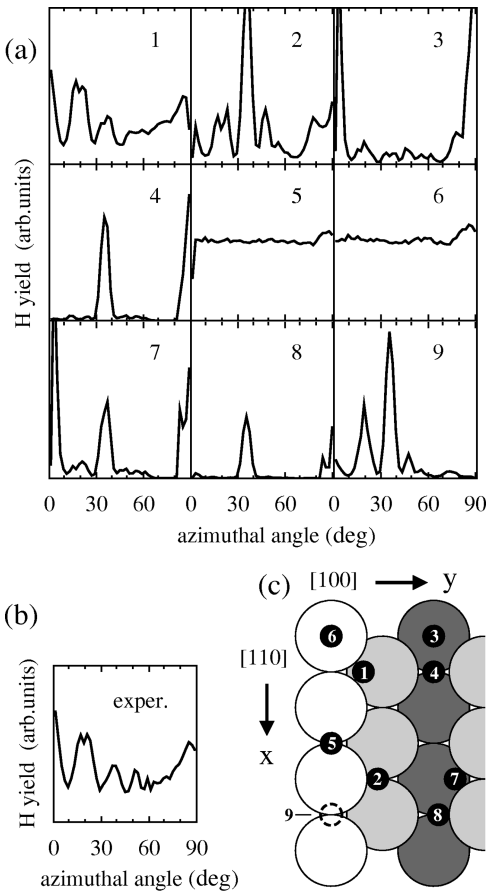

FIG. 5. Calculated H-recoil azimuthal scans (top frame set) for 8 possible on-surface H sites and a subsurface H site compared with the experimental azimuthal scan (bottom frame) for $\alpha=6°$. In the ball-model shown, the x and y axes correspond to the [011] and [100] crystallographic directions, respectively. Azimuthal angles of 0° and 90° correspond to the [100] and [011] crystallographic directions, respectively.

and simulated scans may be due to incomplete 1×2 reconstruction. The background can be caused by surface defects, such as domain boundaries and step edges. The fits obtained confirm that in the 1×2 reconstruction of the Cu(110) surface each second close-packed row is missing. Other surface reconstructions such as 1×3 or 2×4 (Ref. 34) gave very poor fits.

B. Analysis of hydrogen adsorption sites

Figure 5(a) displays calculated H-recoil azimuthal scans for different assumed hydrogen adsorption sites. These sites are indicated in Fig. 5(c) and represent all sites that have been proposed in the quoted literature. They are trigonal hollow sites (1 and 2), a short-bridge hollow site (5), an on-top site (6), deep-trough sites (3, 4, 7, and 8), and a subsurface site (9). The measured azimuthal scan is displayed in Fig. 5(b). It can be easily seen that only for the trigonal hollow sites 1 we obtained a simulated scan resembling the experimental scan. Since the presence and positions of LEIS features are very sensitive to the relative position of atoms at the surface, the obtained data show unambiguously the trigonal hollow site 1 as the main hydrogen adsorption site.

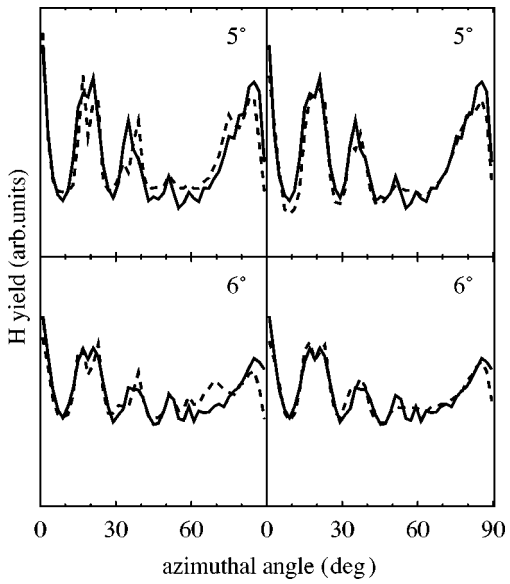

FIG. 6. Fits of the calculated H-recoil azimuthal scans (dashed line) to the experimental scans (solid line) for different thermal vibration amplitudes of H atoms: $\alpha=5°$ (top frames), $\alpha=6°$ (bottom frames); amplitudes calculated from Ref. 2 assuming harmonic type of vibrations (left-hand frames), and amplitudes found in this work to give the best fit (right-hand frames). Azimuthal angles of 0° and 90° correspond to the [100] and [011] crystallographic directions, respectively.

C. Thermal vibration of H

In our simulations, thermal vibrations were included by assuming displacements from the equilibrium positions of the atoms in the x, y, and z directions. The displacements were chosen at random from uncorrelated Gaussian thermal displacement distributions. The width of the distributions for H was treated as a variable. In EELS studies of hydrogen adsorption on the Cu(110) surface, three energy-loss peaks were observed and attributed to three modes of hydrogen vibration in a threefold hollow site.[11] Assuming harmonic vibrations of a H atom in the potential well of an isolated HCu_3 complex, the energy losses correspond to $\Delta E_i=\hbar\omega_i$, where i designates a vibration mode. From these experimental data we calculated the widths of the ground-state vibration amplitude distribution to be 0.12 Å for the vibration mode parallel to the [011] crystallographic direction in the surface plane (along the x axis), 0.13 Å for the vibration mode parallel to the [100] crystallographic direction in the surface plane (along the y axis), and 0.15 Å for the vibration mode perpendicular to the surface plane (along the z axis). However, to obtain a relatively good fit of a calculated H-recoil azimuthal scans to the measured data we had to use much larger thermal vibration amplitudes of the H atoms, namely 0.34, 0.37, and 0.43 Å, respectively. The results of computer simulations carried out for both sets of amplitudes and fitted to the experimental scans are given in Fig. 6. The observed large effective vibrations point to a nonharmonic potential, for which the H wave function is more extended than for a harmonic potential. It should be mentioned that our H thermal vibration amplitudes are very close to the value of 0.23 Å found by Foss *et al.*[35] for the same [0.5 monolayer (ML); see below] coverage of D on the Cu(100) surface. The equivalent amplitudes for H would be 0.32 Å if we correct for the difference in the masses. During the past decade, a number of theoretical and experimental studies appeared on the quantum delocalization of hydrogen on metal surfaces.[7–9,20,36,37] The main conclusion of these works is that the potential well contains important anharmonic components that result in a high mobility of H atoms on the metal surfaces studied. Our observations support these conclusions for Cu(110).

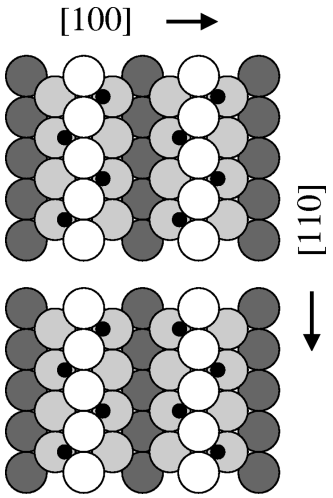

FIG. 7. Geometry of the surface: 0.5-ML H coverage with a symmetric arrangement (top) and an antisymmetric arrangement (bottom).

D. Different coverages and symmetries

From our experiments, a direct determination of the absolute hydrogen coverage from the H peak contents was not possible. However, in the simulations of the H azimuthal scans the coverage was varied to obtain a better fit. The calculations were done for coverages $\theta_H=1.00$, 0.50, and 0.25 ML. Hereby, 1 ML implies two H atoms per one Cu atom in the first ''missing-row'' copper layer. For $\theta_H=0.50$ and 0.25 we considered two different symmetries of the hydrogen atomic arrangement, as illustrated in Fig. 7. Contrary to the Ar or Cu trajectories, the H trajectories are influenced by the presence of other H atoms. The best fit was found for an antisymmetric arrangement with 0.5-ML coverage. A coverage of 0.5 would also be in agreement with recent values given in the literature (see Ref. 10 and references therein). It is probable that the actual coverage of the sample deviates locally from the assumed 0.5 ML. This may cause a slight misfit with the simulations.

E. Buckling

Since in adsorption processes reconstruction of a surface often results in buckling of layers or atomic rows,[38–40] we studied in our computer simulations a possible buckling of the topmost copper rows in directions both perpendicular to the surface and in the plane of the surface. The buckling was obtained by shifting the equilibrium positions of Cu atoms. These shifts did not improve the obtained fits. For larger shifts (>0.1 Å) the features of the simulated azimuthal scans started deviating from the measured LEIS features indicating the absence of any significant displacement of atoms both along and perpendicular to the surface.

F. Location of H: (x,y,z) coordinates

Finally, we studied the interatomic distances between Cu and H atoms. The x, y, and z coordinates of H atoms with respect to a first layer Cu atom were independently varied to improve the agreement between calculated and measured azimuthal scans. The obtained values are listed in Table I. The value $x=1.28$ Å corresponds to the center plane between the two adjacent Cu atoms in the [011] row of the first layer; $y=1.09$ Å implies a displacement from the first layer Cu[011] row towards the trough formed by the missing Cu[011] row and $z=0.08$ Å means that the H atoms are only slightly above the Cu positions of the first layer. These H positions are in qualitative agreement with theoretical calculations based on the effective-medium theory.[20] There it was found that the trigonal hollow site is the most stable H position on a Cu(110)-(1×2) missing-row reconstructed surface. However, the predicted coordinates ($y=1.27$ Å and $z=0.70$ Å) do not agree with our measured values. The measured H position is much deeper into the threefold hollows formed by the first- and second-layer Cu atoms. Our values are closer to those obtained from *ab initio* calculations by Forni *et al.*[41] If we translate their coordinates for the H atom in the threefold hollow site of Cu(111) to the similar site on Cu(110), we find $y=1.10$ Å and $z=0.27$ Å. Our result for the H site on Cu(110)-(1×2) is similar to that found by Bu *et al.*[22] for H on Ni(110)-(1×2). In their LEIS study, H was also found in the trigonal hollow site, located at $y=1.56$ Å from the topmost Ni row and at $z=0.21$ Å above the surface Ni plane. The position determined in our work implies H-Cu distances of 1.68 ± 0.05 Å between a H atom and the nearest first-layer Cu atom and 1.54 ± 0.09 Å between a H atom and the nearest second-layer Cu atom, which are somewhat shorter than the value of 1.70 Å determined by Forni *et al.*[41] In the case of Ni(110)-(1×2)-H system, the distances were found to be 2.0 Å and 1.5 Å, respectively.[22]

IV. CONCLUSION

We performed LEIS studies of the H-covered Cu(110) surface. Our measurements showed unambiguously that the observed 1×2 reconstruction is of the missing-row type as was found earlier. It was shown that the H atoms occupy the trigonal site formed by one second-layer atom and two first-layer Cu atoms. To obtain good fits of the experimental and calculated results, very large thermal vibration amplitudes of H atoms had to be assumed, which is evidence for a nonharmonic potential of H atoms on this surface, giving rise to ''quantum delocalization.'' [5–9] Such a delocalization may point to a high mobility of the H atoms on the Cu(110)-(1×2) surface. The best fits were found for 0.5-ML coverage with an antisymmetric zigzag arrangement of H atoms along close-packed Cu rows. No surface buckling for Cu atoms in the topmost rows was detected with atom displacement larger than 0.1 Å. The interatomic distances between Cu and H atoms were determined.

*Author to whom correspondence should be addressed. FAX: 31 50 363 3471. Electronic address: A.Mijiritskii@phys.rug.nl

†Present address: IKS, University of Leuven, Celestijnenlaan 200 D, B-3001, Leuven, Belgium.

[1] J. B. C. Cobb *et al.*, J. Catal. **164**, 268 (1996).

[2] L. Schlapbach, in *Hydrogen in Intermetallic Compounds II*, edited by L. Schlapbach, Topics in Applied Physics Vol. 67 (Springer-Verlag, Berlin, 1992).

[3] T. Miyake, H. Petek, K. Takeda, and K. Hinode, Appl. Phys. Lett. **70**, 1239 (1997).

[4] R. A. Andrel, B. F. Holland, and G. R. Longhurst, J. Nucl. Mater. **176/177**, 683 (1990).

[5] O. Grizzi *et al.*, Phys. Rev. Lett. **63**, 1408 (1989).

[6] K. Christmann, Surf. Sci. Rep. **9**, 1 (1988).

[7] C. Astaldi, A. Bianco, S. Modesti, and E. Tosatti, Phys. Rev. Lett. **68**, 90 (1992).

[8] M. J. Puska *et al.*, Phys. Rev. Lett. **51**, 1081 (1983).

[9] N. Takagi *et al.*, Phys. Rev. B **53**, 13 767 (1996).

[10] U. Bischler *et al.*, Phys. Rev. Lett. **70**, 3603 (1993).

[11] B. E. Hayden, D. Lackey, and J. Schott, Surf. Sci. **239**, 119 (1990); M. Rohwerder and C. Benndorf, *ibid.* **307–309**, 789 (1994).

[12] K. H. Rieder and W. Stocker, Phys. Rev. Lett. **57**, 2548 (1986).

[13] W. Eberhardt, F. Greuter, and E. W. Plummer, Phys. Rev. Lett. **46**, 1085 (1981).

[14] F. Greuter and E. W. Plummer, Solid State Commun. **48**, 37 (1983).

[15] J. T. Yates, C. H. F. Peden, J. E. Houston, and D. W. Goodman, Surf. Sci. **160**, 37 (1985).

[16] P. Hofmann and D. Menzel, Surf. Sci. **152/153**, 382 (1985).

[17] M. Lagos and I. K. Schuller, Surf. Sci. **138**, L161 (1984).

[18] C. T. Chan and S. G. Louie, Solid State Commun. **48**, 417 (1983).

[19] R. Spitzl, H. Niehus, B. Poelsema, and G. Comsa, Surf. Sci. **239**, 243 (1990).

[20] K. W. Jacobsen and J. K. Nørskov, Phys. Rev. Lett. **59**, 2764 (1987).

[21] J. K. Nørskov, Surf. Sci. **299/300**, 690 (1994).

[22] H. Bu, C. D. Roux, and J. W. Rabalais, Surf. Sci. **271**, 68 (1992).

[23] G. Dorenbos, M. Breeman, and D. O. Boerma, Phys. Rev. B **47**, 1580 (1993).

[24] M. Breeman, G. Dorenbos, and D. O. Boerma, Nucl. Instrum. Methods Phys. Res. B **64**, 64 (1992).

[25] U. Bischler and E. Bertel, J. Vac. Sci. Technol. A **11**, 458 (1993).

[26] A. V. Mijiritskii, U. Wahl, M. H. Langelaar, and D. O. Boerma, Nucl. Instrum. Methods Phys. Res. B (to be published).

[27] A. Dygo, W. N. Lennard, and I. V. Mitchell, Nucl. Instrum. Methods Phys. Res. B **74**, 581 (1993).

[28] M. H. Langelaar, M. Breeman, A. V. Mijiritskii, and D. O. Boerma, Nucl. Instrum. Methods Phys. Res. B **132**, 578 (1997).

[29] J. F. Ziegler, J. P. Biersack, and U. Littmark, *Stopping Power and Ranges of Ions in Matter* (Pergamon, New York, 1985); D. J. O'Connor and J. P. Biersack, Nucl. Instrum. Methods Phys. Res. B **15**, 14 (1986).

[30] O. S. Oen and M. T. Robinson, Nucl. Instrum. Methods **132**, 647 (1976).

[31] H. Dürr, R. Schneider, and Th. Fauster, Vacuum **41**, 376 (1990).

[32] M. Copel, T. Gustafsson, W. R. Graham, and S. M. Yalisove, Phys. Rev. B **33**, 8110 (1986).

[33] A. P. Baddorf, I.-W. Lyo, E. W. Plummer, and H. L. Davis, J. Vac. Sci. Technol. A **5**, 782 (1987).

[34] V. Penka, K. Christmann, and G. Ertl, Surf. Sci. **136**, 307 (1984).
[35] M. Foss, F. Besenbacher, C. Klink, and I. Stensgaard, Chem. Phys. Lett. **215**, 535 (1993).
[36] D. R. Hamann, J. Electron Spectrosc. Relat. Phenom. **44**, 1 (1987).
[37] D. R. Hamann and P. J. Feibelman, Phys. Rev. B **37**, 3847 (1988).
[38] M. P. Bessent, P. Hu, A. Wander, and D. A. King, Surf. Sci. **325**, 272 (1995).
[39] T. Ohno and K. Shiraishi, Solid State Commun. **92**, 397 (1994).
[40] S. Jeong and M. H. Kang, Phys. Rev. B **54**, 8196 (1996).
[41] A. Forni, G. Wiesenekker, E. J. Baerends, and G. F. Tantardini, J. Phys.: Condens. Matter **7**, 7195 (1995).